Article ID: 1006-8775(2011) 04-0430-11

IMPACT OF LATENT HEAT FLUX ON INDIAN SUMMER MONSOON DURING EL NIÑO/LA NIÑA YEARS

M. V. Subrahmanyam (苏伯拉曼雅姆), WANG Dong-xiao (王东晓)

(State Key Laboratory of Tropical Oceanography, Chinese Academy of Sciences, Guangzhou 510301 China)

Abstract: El Niño or La Niña manifest in December over the Pacific and will serve as an index for the forecasting of subsequent Indian summer monsoon, which occurs from June to mid-September. In the present article, an attempt is made to study the variation of latent heat flux (LHF) over the north Indian Ocean during strong El Niño and strong La Niña and relate it with Indian monsoon rainfall. During strong El Niño the LHF intensity is higher and associated with higher wind speed and lower cloud amount. During El Niño all India rainfall is having an inverse relation with LHF. Seasonal rainfall is higher in YY+1 (subsequent year) than YY (year of occurrence). However there is a lag in rainfall during El Niño YY+1 from June to July when compared with the monthly rainfall.

Key words: latent heat flux; Southwest Monsoon; All India Rainfall; El Niño; La Niña

CLC number: P46 **Document code:** A **doi:** 10.3969/j.issn.1006-8775.2011.04.013

1 INTRODUCTION

El Niño is an abnormal warming of sea surface waters of Pacific Ocean off the coast of Peru. It is having profound influence on the global circulation patterns and subsequent economy of not only the nearby country Peru but also having influence globally, especially on far away Asian Summer Monsoon. The failure of Asian Summer Monsoon affects the economy and agriculture production of countries like India and China. On the contrary cooling and reduction of Sea Surface Temperature (SST) is termed as La Niña (opposite of El Niño). El Niño is closely associated with Southern Oscillation and is termed as El Niño and Southern Oscillations (ENSO). However it is also found that the El Niño is irregular and aperiodic[1]. During El Niño years the Walker circulation is altered due to the changes in the Pacific Ocean. During El Niño the lifting and sinking of air—and therefore rainy and dry conditions—move with the warmer and colder SSTs to form the pattern in the Pacific Ocean and the atmosphere. Asymmetries between the life cycles of atmosphere–ocean phenomena during warm and cold episodes have been documented in detail by Larkin and Harrison[2]. El Niño growth is further enhanced by a subsequent warm Kelvin wave in boreal summer, which is driven by the anomalous westerlies related to surface cooling and downdraft air over the eastern pole of the growing Indian Ocean Dipole (IOD)[3]. Recent model studies suggested that the Indian Ocean climate variability might have important influence on the Pacific ENSO variations and frequency[4-6].

Indian monsoon systems are driven by air-sea interaction. The southeast trade wind belt of west Australia, the Bay of Bengal and the Arabian Sea are of particular interest in the Indian Ocean regime. The predominant phenomenon found in the Indian Ocean region is the annual monsoon reversal. In general, the summer monsoon in the lower atmosphere is dominated by strong westerly and southwesterly flow. Strong cross-equatorial flow is observed along the east coast of Africa in association with the low-level Somali jet or Findlater Jet[7]. This cross-equatorial flow is the likely mechanism that transports moisture from the southern Indian Ocean into the Arabian Sea[8]. Slingo and Annamalai[8] further suggested that the monsoon system might reside in distinct circulation regimes depending on the intensity of ENSO events.

Monsoons are predominately characterized by their overall flow patterns. Evaporation over the oceans guided by the factors like radiation balance

Received 2010-06-07; **Revised** 2011-09-02; **Accepted** 2011-10-15
Foundation item: Key Project of Chinese National Programs for Fundamental Research and Development (973 program) (2011CB403500, 2011CB403504)
Biography: WANG Dong-xiao, Professor, Ph.D., primarily undertaking research on air-sea interaction.
Corresponding author: WANG Dong-xiao, e-mail: dxwang@scsio.ac.cn

and the flux of evaporation depends on SST and wind speed. Shukla and Nisra[9] found that higher wind speeds over the Arabian Sea are correlated with lower SST. The stronger winds lead to increase in evaporation as well as increase in upwelling, which results in extension of cold coastal waters. The important role of wind-induced variations of latent heat transfer in warming of the southern Indian Ocean has been noted in observational study by Yu and Reinecker[10]. Warmer SST over the Indian Ocean in the summer is responsible for weak atmospheric circulation, which is found during a dry monsoon period. Conversely, colder SST is responsible for stronger atmospheric forcing during a wet monsoon. However the relation between SST and rainfall is weak[11]. Verma[12] suggested that the warm phase of ENSO is associated with weaker monsoon activity, on the other hand the cool phase of ENSO results in strong monsoon activity, and subsequently, the monsoon precipitation is less or more respectively. Better estimates of surface fluxes as well as their uncertainty will permit a determination of importance of fluxes between the atmosphere and upper ocean thermodynamics. Some studies have tested the relationship between the fluxes and SST fields over broad scale which indicates anomalous heating by the surface fluxes. The fluxes are major components in producing monthly thermal anomalies in the Northern Hemispheric oceans. Some correlation has been established between Indian Ocean LHF and rainfall, including observational studies and an ocean general circulation model[13-16]. Wind surges over the Arabian Sea get intensified and occupy a larger area for warmer SSTs. This increases the evaporation-induced convection over Arabian Sea, leading to increase in precipitation. A critical SST beyond which winds do not intensify further and precipitation does not increase[17] is the saturation SST. It is of interest to note that the latent heat lost by the ocean to the atmosphere is of critical importance to the atmosphere.

The Northern Indian Ocean is an important area to study the monsoon system. Oceanic LHF is one parameter for better understanding of the monsoons and varies with different global phenomena like El Niño and La Niña. This study covers Arabian Sea (5° S to 20° N and 45° E to 80° E), which is significant for the southwest monsoon and contributes the rainfall to the whole Indian subcontinent during summer monsoon period. Over the Arabian Sea wind speed is playing a dominant role during the southwest monsoon and is the main factor affecting LHF while the effect of SST is not as much as that of wind.

2 DATA AND METHODOLOGY

The classification of El Niño and La Niña periods are obtained based on Nino 3.4 index. The Oceanic Nino Index (ONI) has become the de-facto standard that the NOAA uses for identifying El Niño (warm) and La Niña (cool) events in the tropical Pacific using the 3-month running mean of SST anomalies for the Nino 3.4 region[18]. Events are defined as five consecutive months at or above +0.5 anomalies for warm (El Niño) events and at or below -0.5 anomalies for cold (La Niña) events. The threshold is further broken down into Weak (with a 0.5 to 0.9 SST anomaly), Moderate (1.0 to 1.4) and Strong (≥ 1.5) events in terms of magnitude. For the purpose of reporting for an event to be weak, moderate or strong, it must have equaled or exceeded the threshold for at least three months. (For the present analysis, we used monthly LHF, wind, momentum flux and SST data from NCEP-NCAR reanalysis data[19] (2.5° latitude-longitude grid) for the strong El Niño and La Niña years in the period 1950–2006. The cloud amount (with a resolution of 1° ×1°) data are obtained from the International Comprehensive Ocean-Atmosphere Data Set (ICOADS) and the all India monthly rainfall data from the Indian Institute of Tropical Meteorology (IITM), Pune, India during the same period. Over the study area spatial distribution of composite mean monthly anomalies of LHF, SST and wind are plotted separately for all the monsoon months of strong El Niño and strong La Niña for the year of occurrence (YY) and subsequent year (YY+1). Further the LHF mean monthly anomalies are compared with the all India rainfall anomalies to identify the relationship between them.

The LHF is very much dependent on wind speed, SST, evaporation etc. In order to obtain the relationship between wind speed and LHF, we altered the wind speed in the formula given below:

$$\mathrm{LHF} = \rho\, L_v\, C_E\, U\, (q_0 - q_{10})$$

where ρ is the air density, L_v the latent heat of vaporization, C_E the evaporation coefficient, U the wind, q_0 the saturation specific humidity at surface and q_0 is q at the height of 10 m.

LHF has been obtained from different values of wind speed to observe the sensitivity and dependence. The variation of LHF for different wind speeds are verified and presented.

3 RESULTS

The mean spatial distribution of LHF anomalies (LHFA) are presented in Figs. 1 and 2 during strong El Niño and strong La Niña for the monsoon months of June to September (JJAS) in YY and YY+1. A close examination of LHFA reveals that LHFA is very important in characterizing strong El Niño and

strong La Niña. Fig. 1 explains the spatial distribution of LHFA during the monsoon months of YY and YY+1 of strong El Niño. June of YY exhibits negative anomalies over the Somali coast and also near the Indian coast. The anomalies in lower latitudes and near the equator are positive. Positive LHFA in June of YY+1 can be seen over the Somali coast with a maximum of >30 W/m², which is a different scenario from June of YY. Anomalies are negative in the northern Arabian Sea but positive near the Indian coast. LHFA is higher during YY+1 than in YY over the Arabian Sea. All over the Arabian Sea positive LHFA is shown in July of YY. In the southern Arabian Sea LHFA is weak. In the northern Arabian Sea the anomalies are positive and stronger in magnitude. July of YY+1 displays higher LHFA over the Somali coast (>45 W/m²) which is extending towards the Indian coast. July of YY+1 shows higher positive anomalies than YY, including June of YY+1. August of YY displays a decrease in anomalies over the Somali coast. However there is an increase of positive anomalies near the Indian coast, though the positive anomalies are higher during YY+1. August of YY+1 displays higher positive anomaly of >25 W/m² over the Somali coast. September of YY shows positive anomalies in the northern Arabian Sea; however in the central Arabian Sea anomalies are negative. Positive anomalies are present in the northern Arabian Sea and near the Indian coast during September of YY+1. From the above mentioned scenario, LHFA is higher during YY+1 than YY even as it extends till September in YY+1.

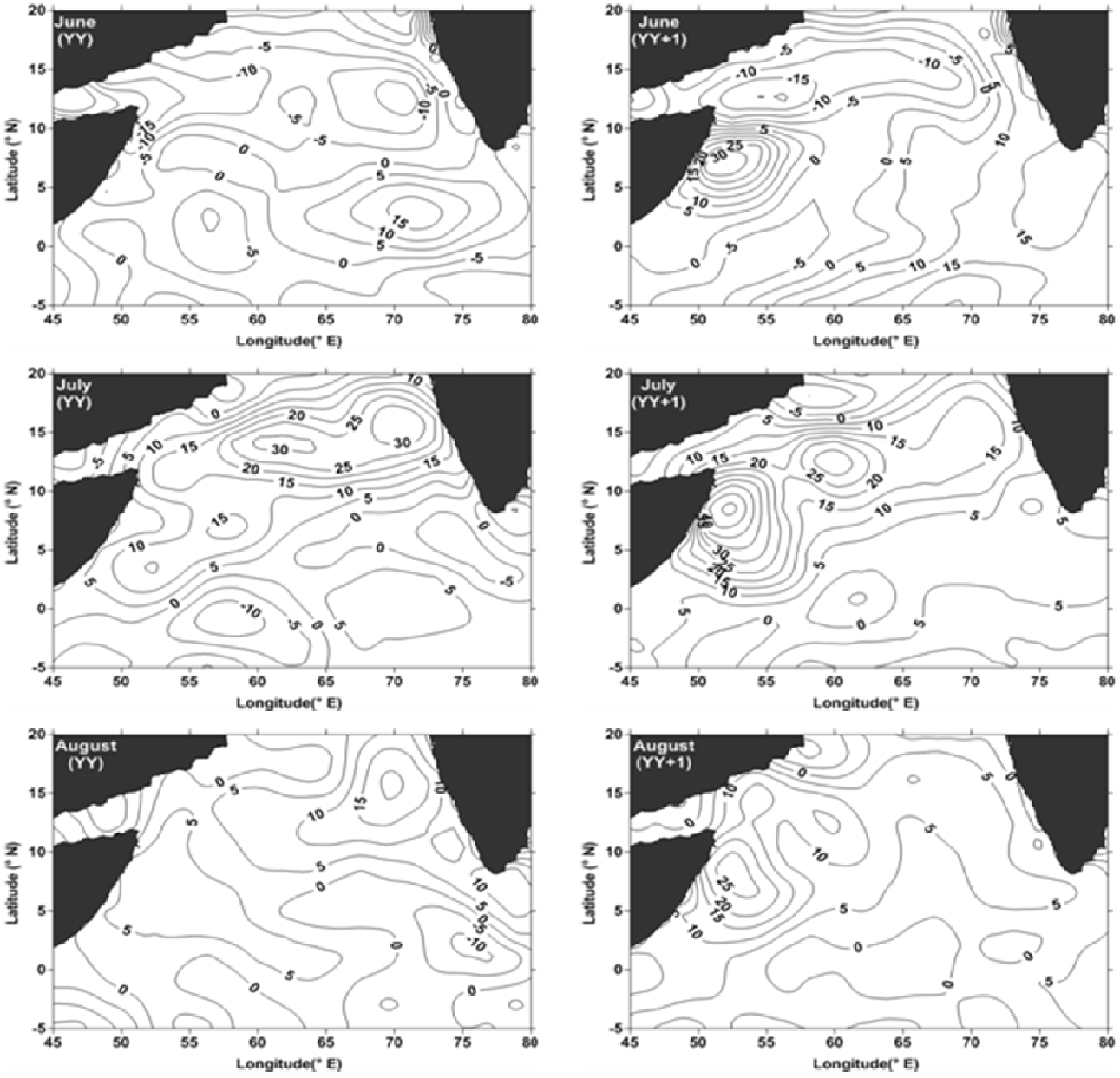

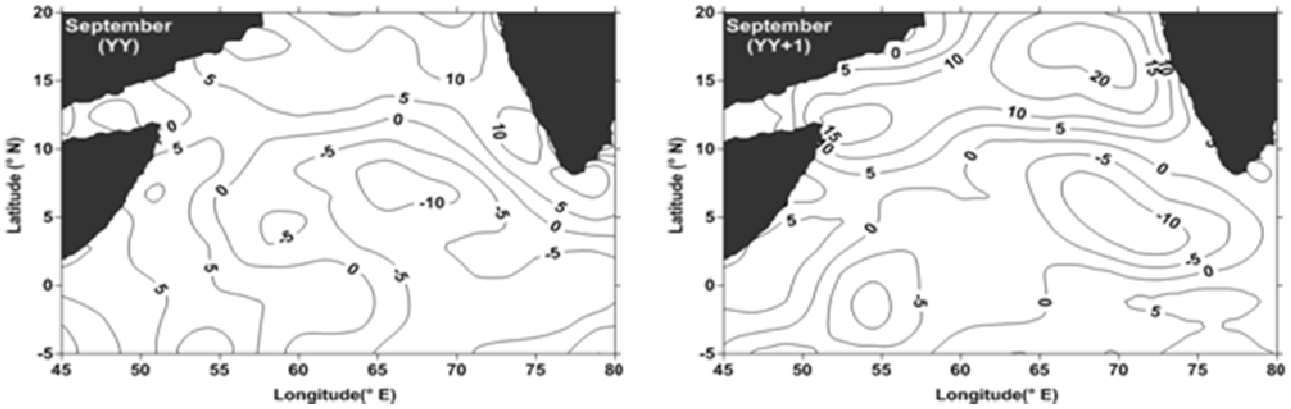

Fig. 1. Mean variation of LHF anomalies during the monsoon months of El Nino over Arabian Sea. Left panel presents the variation of LHF during YY and right panel presents the variation of LHF during YY+1 of different months (JJAS) of monsoon.

Spatial distribution of mean LHFA for strong La Niña during the monsoon months is presented in Fig. 2. LHFA in June of YY is positive at the Somali coast, which differs from the anomalies of El Niño. Over the Arabian Sea LHFA is negative during El Niño and positive during La Niña, while the central Arabian Sea displays negative and positive values over the northern Arabian Sea in June of YY+1. Larger negative anomalies (<-30 W/m²) are present at the Somali coast and extend towards the southern Indian coast with a decrease in intensity. In July of YY, LHFA is larger at the Somali coast and normal at the Indian coast. In July of YY+1 LHFA is relatively normal over the Somali coast and also at the Indian coast. However, LHFA exhibits positive at the southern and negative at the northern coast off Somali, whereas northern Arabian Sea displays positive anomalies. August of YY shows positive LHFA near the Somali coast and normal at the Indian coast. In September of YY, LHFA is positive at the northern Somali coast and normal over the Somali coast and also at the Indian coast. In September of YY+1, lower LHFA can be found at the Somali coast, normal LHFA at the Indian coast and negative LHFA at the southern Indian coast. During El Niño the rainfall is erratic, though sometimes may be normal. However, the distribution explains that rainfall is much lower in June and sometimes has a gap in August. It is this earlier failure of monsoon in the month of June and large gaps in intraseasonal scale that typically affects the rainfall distribution and subsequent agricultural crop pattern. In contrast to El Niño, the rainfall in La Niña is always excessive. Over all, one can comment that the oscillation in LHF, both in time and in intensity, is very large during strong El Niño periods. However, such oscillation in LHF is not observed during strong La Niña periods.

The mean spatial distribution of wind anomalies and SST anomalies during strong El Niño are determined (figure omitted). Winds in June of YY clearly indicate that there is a strong wind field over the Indian Ocean, which is westerly between 60–80° E and easterly between 40–60° E. The wind is northerly in the latitudes of 0–20° N and southwesterly at the west coast of India is well established. The superimposed contour of SST illustrates a zonally elongated high between the latitudes of 10–25° N. If we look for the same feature in the same month of YY+1, the vortex is clearly visible at 75° E and 10° N. In fact, in the Indian Ocean the wind is southerly. The typical easterly between 40–60° E is absent. SST anomalies are strong but slightly higher off the Somalia coast. In July the same pattern continues, but the easterly is strong in YY. The southerly component of the wind in the northern Arabian Sea is also clearly visible. The SST displays three typical centers in both figures of July but the areal extent is less in YY+1. In August there is much contrast in the wind fields between YY and YY+1. In YY, wind is easterly in the northern latitudes, which is replaced by strong westerly over the lower latitudes and typically, strong westerly momentum is absent at the equator. In YY+1, wind is westerly as the wind is following from the Arabian Sea to the Bay of Bengal. Examining the SST anomalies in August of YY shows that there are centers of lower SST anomaly near the equator and off the coast of Somali, with no similar center being found near the Indian coast and the gradient of SST anomaly is southerly. Meanwhile, in YY+1, small low SST anomaly centers are found near the southern tip of the Indian subcontinent. In fact, there are two similar centers near the coast and two off the coast of India. In northern latitudes off the coast of Somalia, both years reveals strong gradient of SST. However, the gradient of SST is more pronounced in YY+1. This is also corroborated by the wind in the northeast direction in YY+1. The wind in September is intense in YY when compared to that of YY+1. The gradient of SST is from north to south.

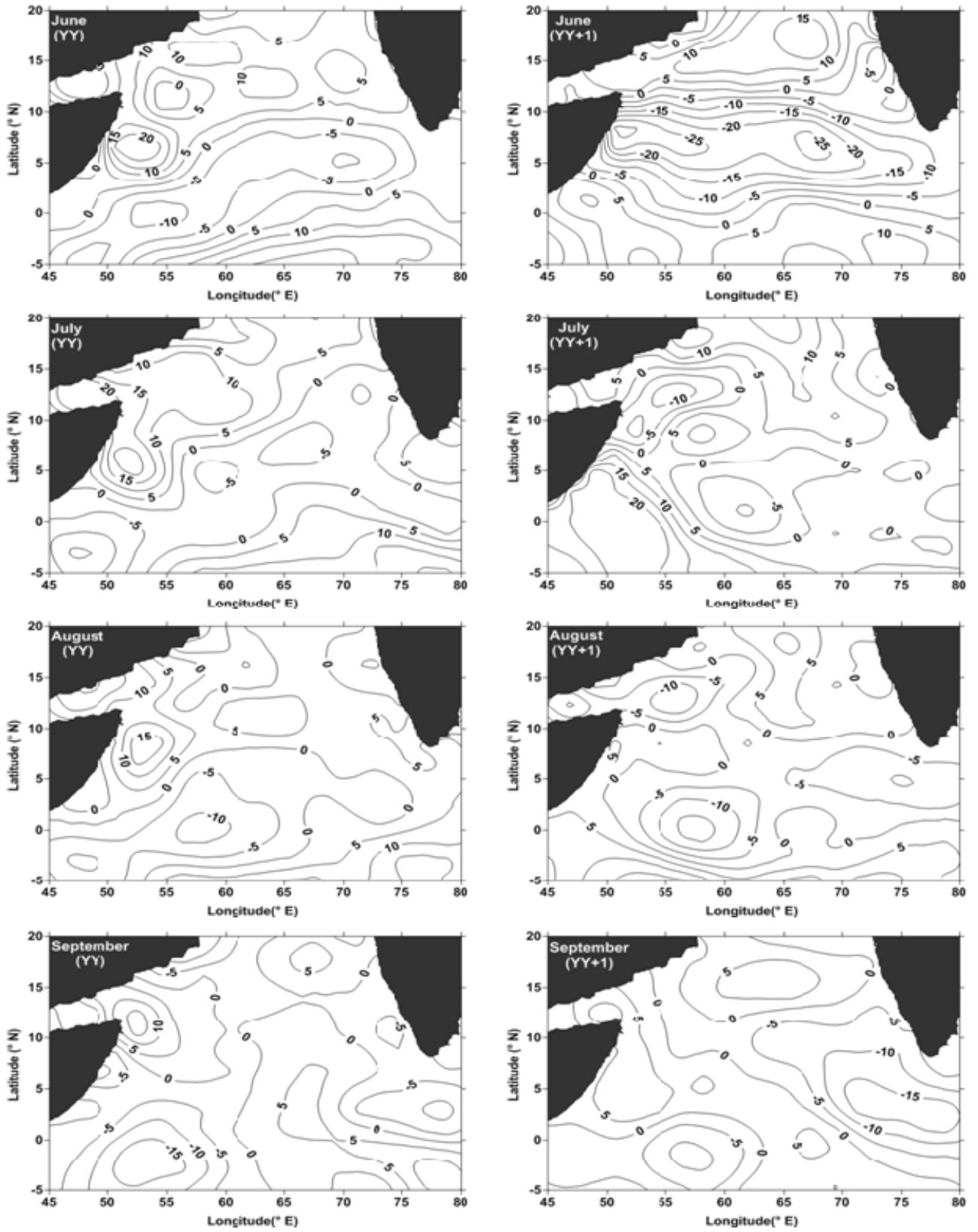

Fig. 2. Mean variation of LHF anomalies during the monsoon months of La Nina over Arabian Sea, left panel presents the variation of LHF during YY and right panel presents the variation of LHF during YY+1 of different months (JJAS) of monsoon.

It is shown from the mean spatial distribution of wind anomalies and SST anomalies during strong La Niña (figure omitted) that wind is strong over the Indian Ocean during June of YY, so there is a lot of momentum flux coming from the east. It is also interesting to note that, there is a strong westerly component at lower latitudes. The wind is turning north and southwest, which hits the west coast of

India. It demonstrates that the monsoon is very active, even though the intensity decreases. However, the same pattern is observed in June of YY+1. The vortex, which centers at 10° N, is typical for June of YY+1. In July, there is also a strong westerly component right up to 50° E. There is a reversal, that is, the easterly component dominates in YY+1. Similarly, in August of YY, there is a westerly component whereas in YY+1 there is an easterly component. During September of YY, the monsoon is still strong as revealed by the southwesterly component hitting the west coast of India. However, such component is absent in YY+1. During strong La Niña, SST in YY exhibits a warm pool in the Indian Ocean. Such a warm pool is not present near the Indian coast. In YY+1 the warm pool is larger in June over lower latitudes and its intensity is higher in July than in June. August shows the same pattern both in YY and YY+1 in the central Arabian Sea. September of YY is worth mentioning; because it has southwesterly wind and two warm pools. In YY+1 the warm pools shift to the east. There is no effect of wind as it is weak.

The variation of mean momentum flux during the El Niño is presented in Fig. 3. In June of YY, a cyclonic momentum can be seen at 5° N and 73° E, whereas it is absent during June of YY+1. Momentum flux shows a typical westerly momentum up to 60° E in August of YY. There is an easterly momentum from 45° E to 60° E in August of YY+1. At 5° N, the momentum flux is southwesterly in August of YY, whereas in YY+1 the momentum flux is weak and vortex is absent. In September of YY+1 momentum flux is towards the south in direction and between 75–80° E.

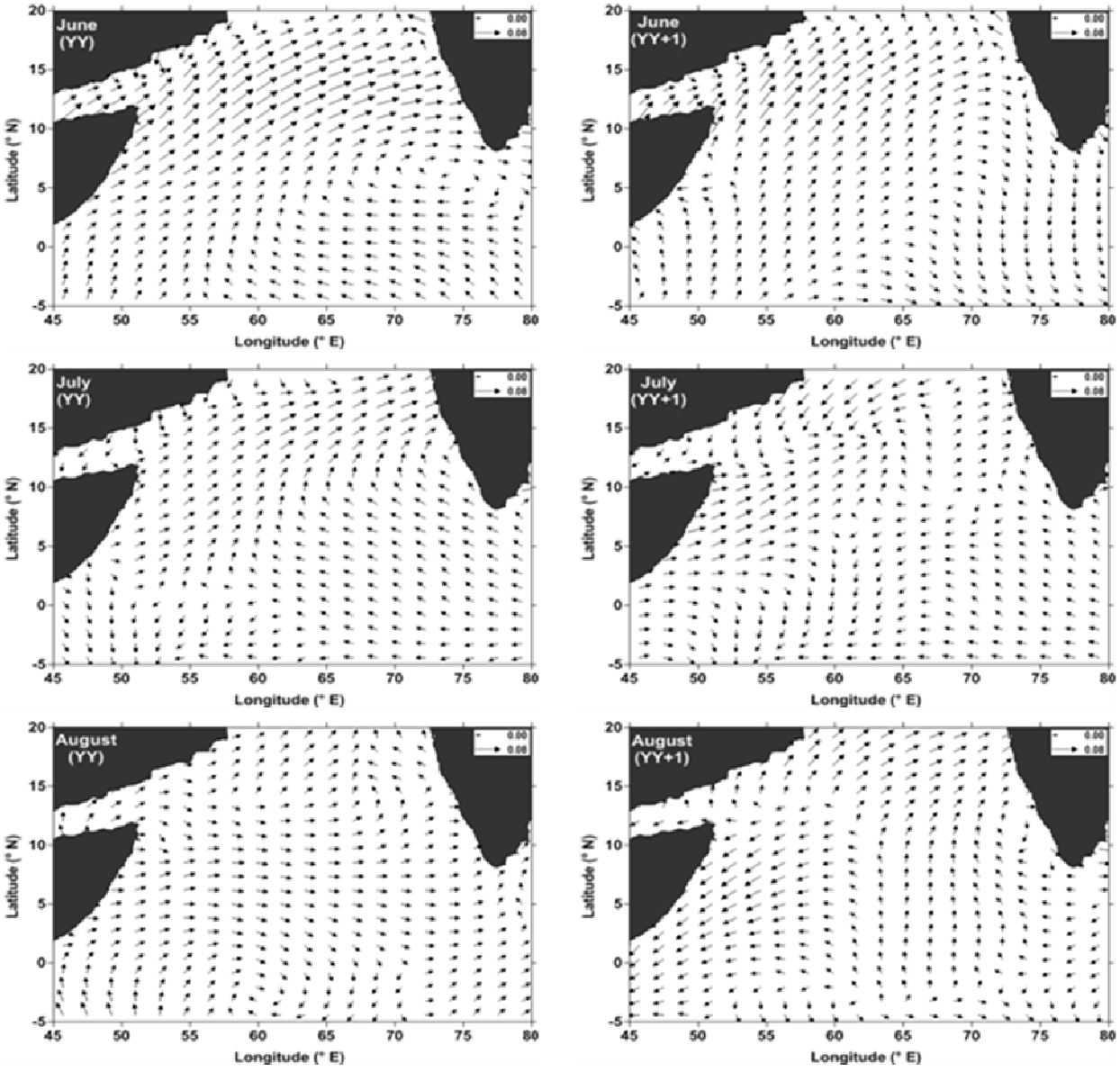

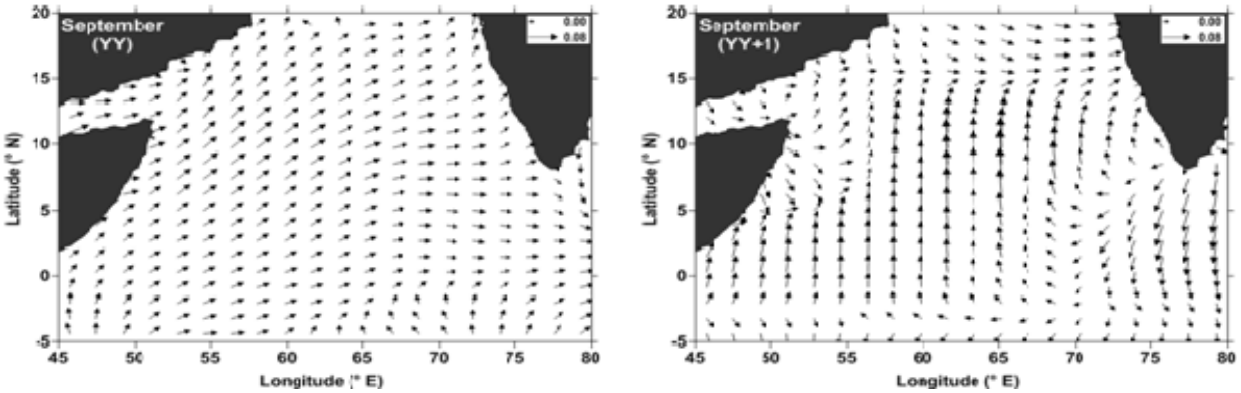

Fig. 3. Mean momentum flux anomalies during the monsoon months of El Niño over Arabian Sea. Left panel represents the variation of momentum flux during YY and right panel represents the variation of momentum flux during YY+1 of different months (JJAS) of monsoon.

The variation of mean momentum flux during La Niña is determined (figure omitted). In July of YY momentum flux is directed towards the Indian coast. However, in northern latitudes there is a northeasterly component. The momentum flux presents a picture showing that it is a part of a bigger cyclonic circulation during June of YY+1, and momentum flux is towards the Bay of Bengal and the westerly component is higher near the equator. Momentum flux is very strong and from the southwest direction, and hits the Indian coast during July of YY, whereas in YY+1, the momentum flux is easterly. The same pattern continues in August of YY but with less intensity and it is towards the Indian coast and the Bay of Bengal during August of YY+1. Momentum flux is westerly in September of YY and towards the India coast and Bay of Bengal. However it is easterly in YY+1.

The mean variation of LHFA over the study area and all India rainfall anomalies are presented in Figs. 4 and 5 for YY and YY+1. Fig. 4a depicts the LHFA for different monsoon months and southwest monsoon seasonal mean (SWM) of YY. It should be mentioned here that during strong El Niño positive anomalies are observed in July and August, whereas anomalies are negative in June and September. However, during strong La Niña negative anomalies are observed with the exception of August. SWM anomaly is positive in strong El Niño and negative in strong La Niña. Fig. 4b depicts the variation of LHFA during YY+1. Positive anomalies can be seen throughout the monsoon months during strong El Niño and negative anomalies during strong La Niña and SWM anomaly also gives the same result.

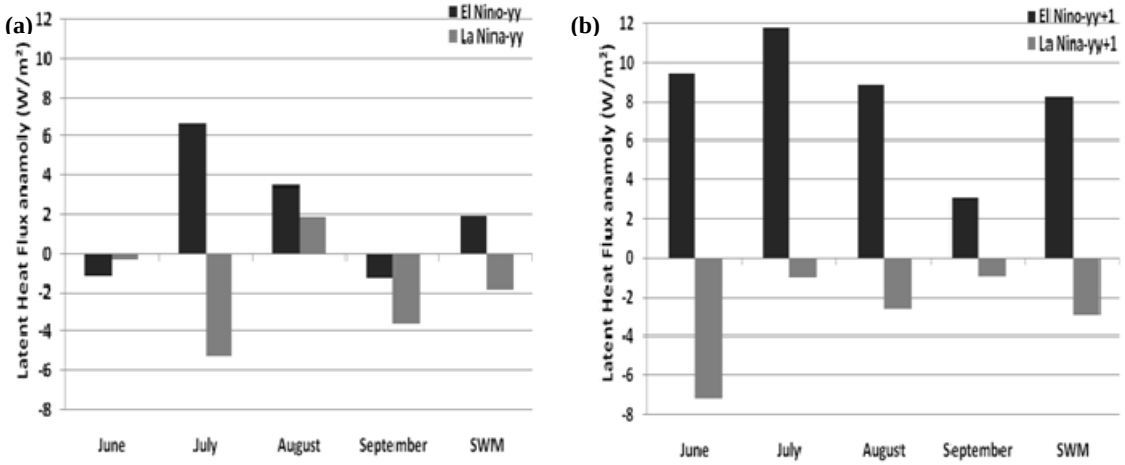

Fig. 4. Mean monthly and southwest monsoon season variations of LHF anomalies during strong El Niño and La Niña in the YY and YY+1 over Arabian Sea. (a) LHF anomaly variations during YY over Arabian Sea. (b) Same as (a) but for YY+1.

The variation of all India rainfall anomalies for YY is given in Fig. 5a. It is observed that strong El Niño is associated with negative rainfall anomaly, however strong La Niña shows positive anomaly. The same pattern is also observed with SWM anomaly. The rainfall anomaly for YY+1 are presented in Fig. 5b. During strong El Niño negative anomaly is observed in June and July, whereas positive anomalies

appear in the following months. During strong La Niña rainfall anomaly is normal in June and then turns positive and becomes higher in July and August before turning negative in September. The SWM anomaly during strong El Niño and strong La Niña are positive. The SWM anomaly is negative during El Niño and positive during La Niña in YY. However, both strong El Niño and strong La Niña reveal positive anomalies in YY+1. As compared to the monthly rainfall anomalies, there is a lag, or a shift, of rainfall during YY+1.

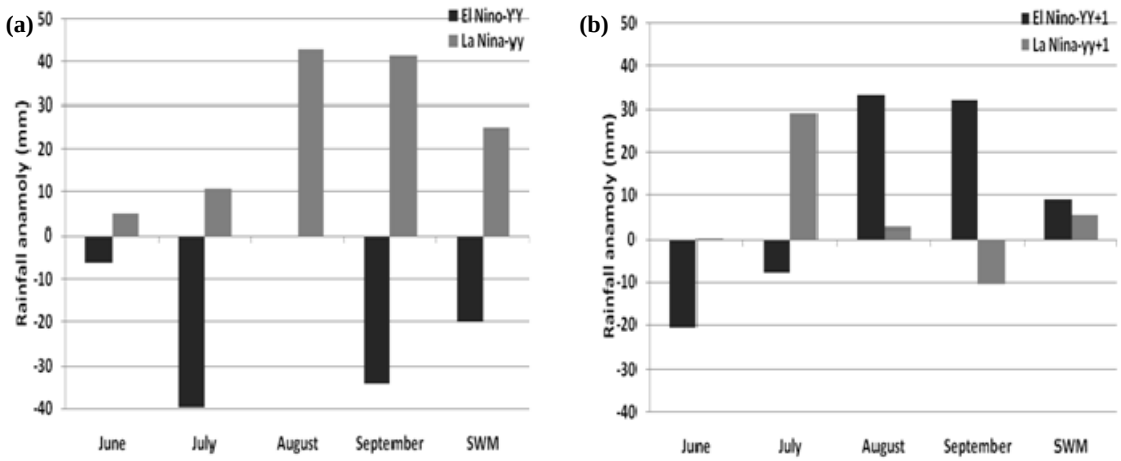

Fig. 5. Mean monthly and southwest monsoon season variations of all India rainfall anomalies during strong El Niño and La Niña in the YY and YY+1 over Indian subcontinent. (a) All India Rainfall anomaly during YY over Indian subcontinent. (b) Same as (a) but for YY+1.

Figure 6 depicts the variation of LHF over the Arabian Sea during the monsoon months and the effect of wind on LHF. When the wind speed is constant (2.5 m/s), the LHF value is very low (right panel of Fig. 6). This reveals that wind during monsoon months is the dominant factor that influences the LHF and subsequent monsoon activity over the Indian subcontinent.

Table 1 exhibits the co-located points of wind and cloud where the maximum LHF is found during monsoon months over the Arabian Sea. The cloud amount is used for comparison. The LHF has an impact on both strong El Niño and La Niña. El Niño is associated with higher LHF than La Niña. During strong La Niña, LHF in YY is higher than that in YY+1. Wind speed during strong El Niño decreases during the June of YY+1 than in YY, and in July and August, wind speed is higher in YY and in September wind speed decreases. If we consider SWM during El Niño, wind speed is higher during YY+1 than in YY. In strong La Niña, wind speed is marginally higher in YY+1 than in YY during SWM and also in all monsoon months. During strong El Niño, cloud amount is lower in all the monsoon months of YY+1 than those of YY. However, during strong La Niña cloud amount is higher in June and July and lower in August and September. If we compare the cloud amount during SWM, the cloud amount in YY+1 is slightly higher than that in YY.

4 DISCUSSIONS

Previous studies[8, 20-21] strongly support the notion of a seasonally persistent rainfall anomaly pattern, which is forced by surface boundary conditions (SST, snow mass etc.) or is an integral part of a low-frequency coupled ocean-land-atmosphere fluctuation. Analysis of the dominant modes of global SST shows a global influence of ENSO[22-23]. Present study reveals as follows: Over the Arabian Sea, the Findlater Jet impact on the LHFA can be seen in Figs. 1 and 2. Monthly mean wind speed anomalies during El Niño are observed to be smaller than those during La Niña (figures omitted), and this is in accordance with the observations made by Halpern and Woiceshyn[24]. Cloud amount is lower where the higher intensities of LHF and wind are (Table 1). It can be explained that when there is a maximum LHF (or evaporation) over the sea, the low-level wind jet (or Findlater Jet) carries the moisture above the sea surface from the source, so there is no evidence of cloud formation, which leads to lower cloud amount observed at that location. Therefore, wind is a dominant factor for higher LHF intensity and lower cloud amount. Heat balance of the surface ocean reveals the dominance of the contributions due to changes in LHF, which exhibits a strong relationship with the anomalous surface wind (Fig. 6).

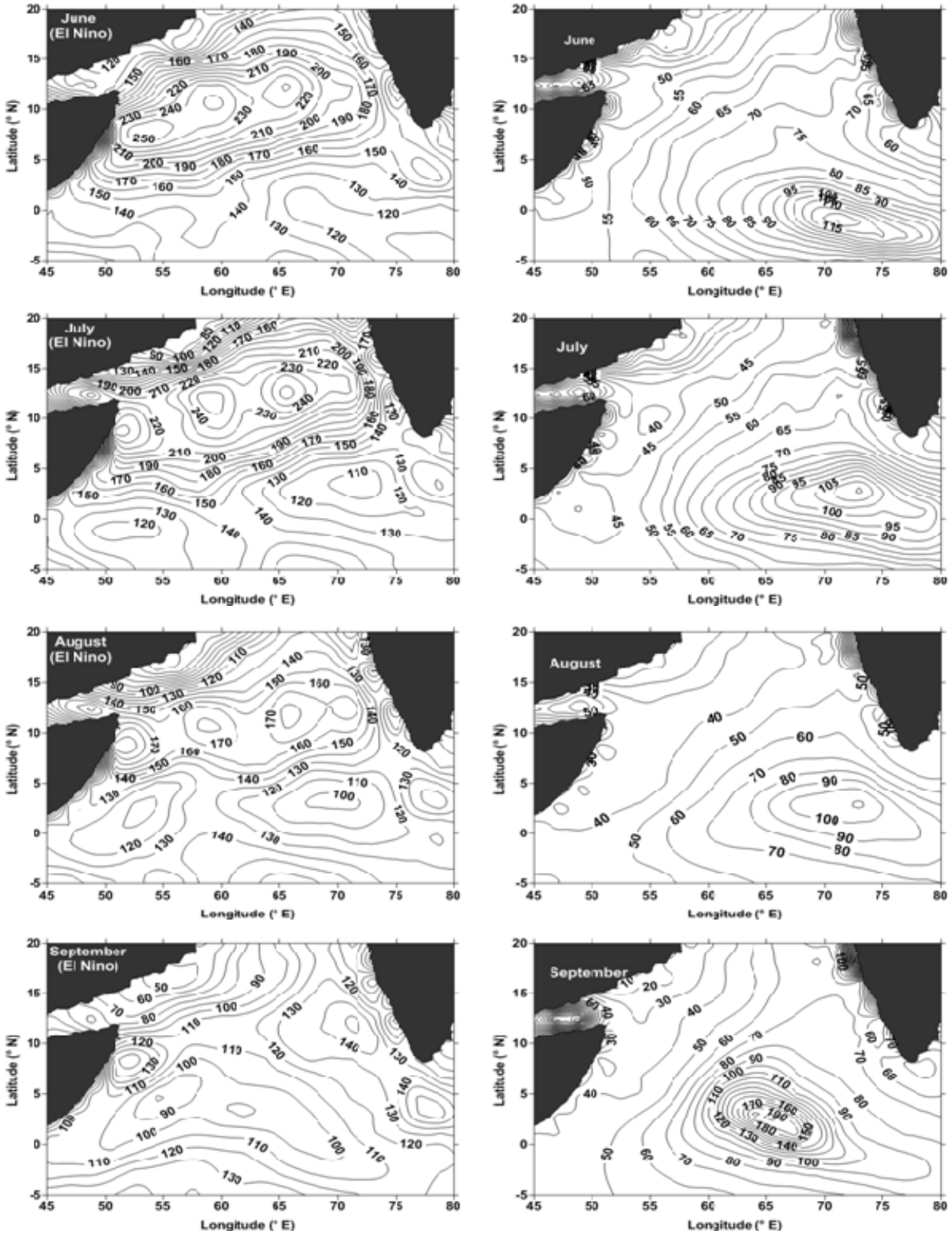

Fig. 6. Mean variation of latent heat flux during monsoon months of El Niño over Arabian Sea, left panel represents the variation LHF with wind speed (actual values) and right panel represents the variation of LHF, where wind speed is constant (2.5m/s) over the Arabian sea to understand how the wind speed affects the LHF.

Summer monsoon covers the Indian subcontinent by the end of June and retrieves in mid-September. We found that LHF is varying with El Niño and La Niña and having an inverse relation with the all India rainfall. Clark et al.[25] mentioned that there is a weaker ENSO signal in the Indian Ocean after 1976 and Fasullo[26] mentioned that strong and neutral ENSO seasons are biennial, which suggest an

increased frequency of deficient seasons being found. During YY of El Niño the seasonal LHFA shows positive and the rainfall is negative, whereas the scenario is the opposite during La Niña (Figs. 4 and 5). When the mean monthly anomalies during YY+1 of El Niño are considered, there is an interesting feature that rainfall lowers in June and then increases to normal in July and is above normal in August and September. It indicates that in YY+1 of El Niño, the rainfall mainly starts from July rather than June. Therefore there is a lag or a shift in rainfall from June to July in YY+1 of El Niño. As this analysis is the composite of strong El Niño and strong La Nina, further studies are needed to verify the effect on Indian summer monsoon rainfall with all the different El Niño and La Nina.

Table 1. The magnitude of the co-located points of cloud amount and wind at the place where the maximum LHF is found.

		Strong El Niño					Strong La Niña				
		Jun.	Jul.	Aug.	Sept.	SWM	Jun.	Jul.	Aug.	Sept.	SWM
YY	LHF (W/m²)	278.6	311.2	238.4	180.1	252.1	273.9	263.6	227.0	168.8	233.3
	Cloud Amount (Oktas)	3.1	2.8	3.3	4.3	3.4	4.3	2.5	4.0	5.5	4.0
	Wind (m/s)	14.2	10.6	12.1	8.5	11.4	13.1	11.1	10.7	5.3	10.1
YY+1	LHF (W/m²)	314.4	338.9	247.9	192.3	273.4	259.1	250.1	209.7	176.9	223.9
	Cloud Amount (Oktas)	3.0	2.3	3.2	4.2	3.2	5.0	5.1	3.9	5.2	4.8
	Wind (m/s)	13.6	12.2	15.4	8.0	12.3	13.3	11.6	11.1	5.9	10.5

5 CONCLUSIONS AND REMARKS

This study clearly indicates that there is a relation between the Arabian Sea LHF and the Indian summer monsoon rainfall. The following important conclusions can be drawn from this study.

(1) LHF is higher during YY+1 than during YY, which means there is sufficient evaporation over the Arabian Sea but the rainfall over the Indian subcontinent is less. There is an inverse relation between LHF and all India rainfall during El Niño (YY and YY+1). However, LHF during La Niña is lower than that during El Niño, but over the Indian subcontinent, rainfall is normal or above normal.

(2) During strong El Niño seasonal rainfall is lower (below normal) in YY and higher (above normal) in YY+1. As for the monthly rainfall during strong El Niño, the rainfall during June is erratic and below normal over the Indian subcontinent; however the rainfall in the other monsoon months (July, August and September) is higher than that in YY. This infers that there is a lag or shift in the rainfall during YY+1 from June to July which extends up to September. This feature cannot be found in the seasonal rainfall. This intraseasonal variation is very important as far as the Indian agriculture is concerned. India is an agricultural country where the sowing operations start in June. However the present study points out that June is the critical month, where the rainfall is below normal rainfall. Therefore, agricultural crops with shorter crop life period and high yield variety should be started in July in case of El Niño (YY+1).

(3) The seasonal rainfall during strong La Niña is always higher in YY than in YY+1.

Acknowledgements: The authors would like to thank IITM and NCEP/NCAR for providing the data. The authors would like to acknowledge Prof. K.P.R Vittalmurthy for valuable discussion and suggestions to improve the manuscript. The authors wish to acknowledge CAS for providing a grant.

REFERENCES:

[1] PHILANDER S G H. El Nino and La Nina [J]. J. Atmos. Sci., 1985, 42: 2652-2662.
[2] LARKIN N K, HARRISON D E. ENSO warm (El Niño) and cold (La Niña) event life cycles: Ocean surface anomaly patterns, their symmetries, asymmetries, and implications [J]. J. Climate, 2002, 15: 1118-1140.
[3] LUO J J, ZHAGN R, BEHERA S K, et al. Interaction between El Niño and Extreme Indian Ocean Dipole [J]. J. Climate, 2010, 23: 726-742. DOI:10.1175/2009JCL13104.1.
[4] BEHERA S K, LUO J J, MASSON S, et al. A CGCM study on the interaction between IOD and ENSO [J]. J. Climate, 2006, 19: 1688-1705.
[5] WU R, KIRTMAN B P. Understanding the impacts of the Indian Ocean on ENSO variability in a coupled GCM [J]. J. Climate, 2004, 17: 4019-4031.
[6] YU L, WELLER R A, LIU W T. Case analysis of a role of ENSO in regulating the generation of westerly wind bursts in the Western Equatorial Pacific [J]. J. Geophys. Res., 2003, 108(C4): 3128.
[7] FINDLATER J A. Major low level air current near the Indian Ocean during the northern summer [J]. Quart. J. Roy.

Meteor. Soc., 1969, 95: 362-380.
[8] SLINGO J M, ANNAMALAI H. 1997: The El Nino of the century and the response of the Indian summer monsoon [J]. Mon. Wea. Rev., 2000, 128: 1778-1797.
[9] SHUKLA J, MISRA B N. Relationships between sea surface temperature and wind speed over the Central Arabia Sea and monsoon rainfall over India [J]. Mon. Wea. Rev., 1977, 105: 998-1002.
[10] YU L S, REINECKER M M. Mechanisms for the Indian Ocean warming during the 1997–98 El Nino [J]. Geophys. Res. Lett., 1999, 26: 735-738.
[11] WEARE C B. Statistical study of the relationship between ocean surface temperatures and the Indian monsoon [J]. J. Atmos. Sci., 1979, 36: 12, 2279-2291.
[12] VERMA R K ENSO—Monsoon linkages as evidenced from Pacific SST correlations with monsoon precipitation [R]. TOGA Notes, 1992, 6: 1-3.
[13] CAYAN D R. Latent and sensible heat flux anomalies over the northern oceans: Driving the sea surface temperature [J]. J. Phys. Oceanogr., 1992, 22: 859-881.
[14] CAYAN D R. Latent and sensible heat flux anomalies over the northern oceans: The connection to monthly atmospheric circulation [J]. J. Climate, 1992, 5: 354-369.
[15] CAYAN D R. Variability of latent and sensible heat fluxes estimated using bulk formulae [J]. Atmos.-Ocean., 1992, 30: 1-42.
[16] FRANKIGNOUL C, REYNOLDS R W. Testing a dynamical model for midlatitude sea surface temperature anomalies [J]. J. Phys. Oceanogr., 1983, 13: 1131-1145.
[17] RAMAN S, ALAPATI K, MADALA RV. Role of the air-sea interaction processes on the Indian Southwest monsoon dynamics, Oceanography of the Indian Ocean [M]// DESAI B N (editor), New Delhi: Oxford & IBH Publishers, 1992, 637-645.
[18] Climate Prediction Center, National Weather Services (USA). Cold and Warm Episodes by Season. http://www.cpc.noaa.gov/products/analysis_monitoring/ensostuff/ensoyears.ERSST.v3.shtml) [2010-06-21].
[19] KALNAY E, COAUTHORS. The NCEP/NCAR 40-Year Reanalysis Project [J]. Bull. Amer. Meteor. Soc., 1996, 77: 437-471.
[20] LANZANTE J R. Lag relationships involving tropical sea surface temperatures [J]. J. Climate, 1996, 9: 2568-2578.
[21] TOURRE Y, WHITE W. ENSO signals in global upper-ocean temperature [J]. J. Phys. Oceanogr., 1995, 25: 1317-1332.
[22] KRISHNAMURTHY V, SHUKLA J. Intraseasonal and interannual variability of rainfall over India [J]. J. Climate, 2000, 13: 4366-4377.
[23] WEBSTER P J, MAGANA V O, PALMER T N, et al. Monsoons: Processes, predictability, and the prospects of prediction [J]. J. Geophys. Res., 1998, 103 (C7): 14451-14510.
[24] HALPERN D, WOICESHYN P M. Somali Jet in the Arabian Sea, El Nino, and India Rainfall [J]. J. Climate, 2001, 14: 434-441.
[25] CLARK O C, COLE J E, WEBSTER P J. Indian Ocean SST and Indian summer rainfall; predictive relationships and their decades variability [J]. J. Climate, 2000, 13: 2503-2519.
[26] FASULLO J. Biennial Characteristics of Indian Monsoon Rainfall [J]. J. Climate, 2004, 17: 2972-2982.

Citation: M. V. SUBRAHMANYAM and WANG Dong-xiao. Impact of latent heat flux on Indian summer monsoon during El Niño/La Niña years. *J. Trop. Meteor.*, 2011, 17(4): 430-440.